

# Chapter 3

## Nonlinear Analyses

### 3.1 Introduction

The method of state space reconstruction was originally proposed by Packard et al. (1980) and formalised by Takens (1981). Since then, various investigations and disciplines relative to nonlinear time series analysis have benefited from it (Aguirre and Letellier, 2009; Frank et al., 2010; Samà et al., 2013; Stergiou and Decker, 2011). The method of state space reconstruction is based on uniform time-delay embedding which is a simple matrix implementation considering the embedding parameters ( $m$  and  $\tau$ ), therefore, matrix represents the reconstruction of an unknown  $d$ -dimensional manifold  $M$  from a scalar time series (e.g. one-dimensional time series in  $\mathbb{R}$ ). A manifold, in this context, is a multidimensional curved surface within a space (e.g. a saddle) (Guastello and Gregson, 2011). Henceforth, The method of state space reconstruction using a scalar time series can preserve dynamic invariants such as correlation dimension, fractal dimension, Lyaponov exponents, Kolmogorov-Sinai entropy and detrended fluctuation analysis (Bradley and Kantz, 2015; Krakovská et al., 2015; Quintana-Duque and Saupe, 2013; Quintana-Duque, 2012, 2016). However, selecting appropriate embedding parameters is still an open challenge.

In the following subsections, we describe in more detail the state space reconstruction theorem (RSSs), uniform time-delay embedding theorem (UTDE), the methods to compute embedding parameters: false nearest neighbours (FNN) and average mutual information (AMI). We also introduce the fundamentals of Recurrence plots(RPs) and Recurrence quantification analysis (RQA).

## 3.2 State Space Reconstruction Theorem

Following the notation employed in Casdagli et al. (1991); Garland et al. (2016); Gibson et al. (1992); Takens (1981); Uzal et al. (2011); Uzal and Verdes (2010), the method of state space reconstruction is defined by:

$$s(t) = f^t[s(0)], \quad (3.1)$$

where  $s, s : A \rightarrow M$  given that  $A \subseteq \mathbb{R}$  and  $M \subseteq \mathbb{R}^d$ , represents a trajectory which evolves in an unknown  $d$ -dimensional manifold  $M$ ,  $f : M \rightarrow M$  is an evolution function and  $f^t$ , with time evolution  $t \in \mathbb{N}$ , is the  $t$ -th iteration of  $f$  that corresponds to an initial position  $s(0) \in M$  (Takens, 1981). Then, a point of a scalar time series  $x(t)$  in  $\mathbb{R}$ , can be obtained with

$$x(t) = h[s(t)], \quad (3.2)$$

where  $h$  is a function,  $h : M \rightarrow \mathbb{R}$ , defined on the trajectory  $s(t)$ .

Reconstructed state space can then be described as an  $n$ -dimensional state space defined by  $y(t) = \Psi[\mathbf{X}(t)]$  where  $\mathbf{X}(t) = \{x(t), x(t - \tau), \dots, x(t - (m - 1)\tau)\}$  is the uniform time-delay embedding with a dimension embedding  $m$  and delay embedding  $\tau$  and  $\Psi : \mathbb{R}^m \rightarrow \mathbb{R}^n$  is a further transformation of dimensionality (e.g. Principal

### 3.3 Uniform Time-Delay Embedding (UTDE)

---

Component Analysis, Singular Value Decomposition, etc) being  $n \leq m$ . With that in mind, uniform time-delay embedding,  $\mathbf{X}(t)$ , defines a map  $\Phi : M \rightarrow \mathbb{R}^m$  such that  $\mathbf{X}(t) = \Phi(s(t))$ , where  $\Phi$  is a diffeomorphic map (Takens, 1981) whenever  $\tau > 0$  and  $m > 2d_{box}$  and  $d_{box}$  is the box-counting dimension of  $M$  (Garland et al., 2016). Then, if  $\Phi$  is an embedding of an attractor (i.e. evolving trajectories) in the reconstructed state space, a composition of functions represented with  $F^t$  is induced on the reconstructed state space:

$$\mathbf{X}(t) = F^t[\mathbf{X}(0)] = \Phi \circ f^t \circ \Phi^{-1}[\mathbf{X}(0)]. \quad (3.3)$$

Hence, an embedding is defined as "a smooth one-to-one coordinate transformation with a smooth inverse" (Casdagli et al., 1991, p. 54). Figure 3.1 illustrates the state space reconstruction.

## 3.3 Uniform Time-Delay Embedding (UTDE)

Frank et al. (2010) and Samà et al. (2013) refer to the state space reconstruction outlined in 3.2 as "time-delay embeddings" or "delay coordinates", respectively. However, we consider the term "uniform time-delay embedding" as more descriptive and appropriate terminology for this thesis.

The uniform time-delay embedding is represented as a matrix of uniform delayed copies of the time series  $\{\mathbf{x}_n\}_{n=1}^N$  where  $N$  is the sample length of  $\{\mathbf{x}_n\}$  and  $n$  is index for the samples of  $\{\mathbf{x}_n\}$ .  $\{\mathbf{x}_n\}_{n=1}^N$  has a sample rate of  $T$ . The delayed copies of  $\{\mathbf{x}_n\}$  are uniformly separated by  $\tau$  and represented as  $\{\tilde{\mathbf{x}}_{n-i\tau}\}$  where  $i$  goes from  $0, 1, \dots, (m - 1)$  (Fig 3.2).  $\{\tilde{\mathbf{x}}_{n-i\tau}\}$  contains information of unobserved state variables and encapsulates the information of the delayed copies of the available time series in

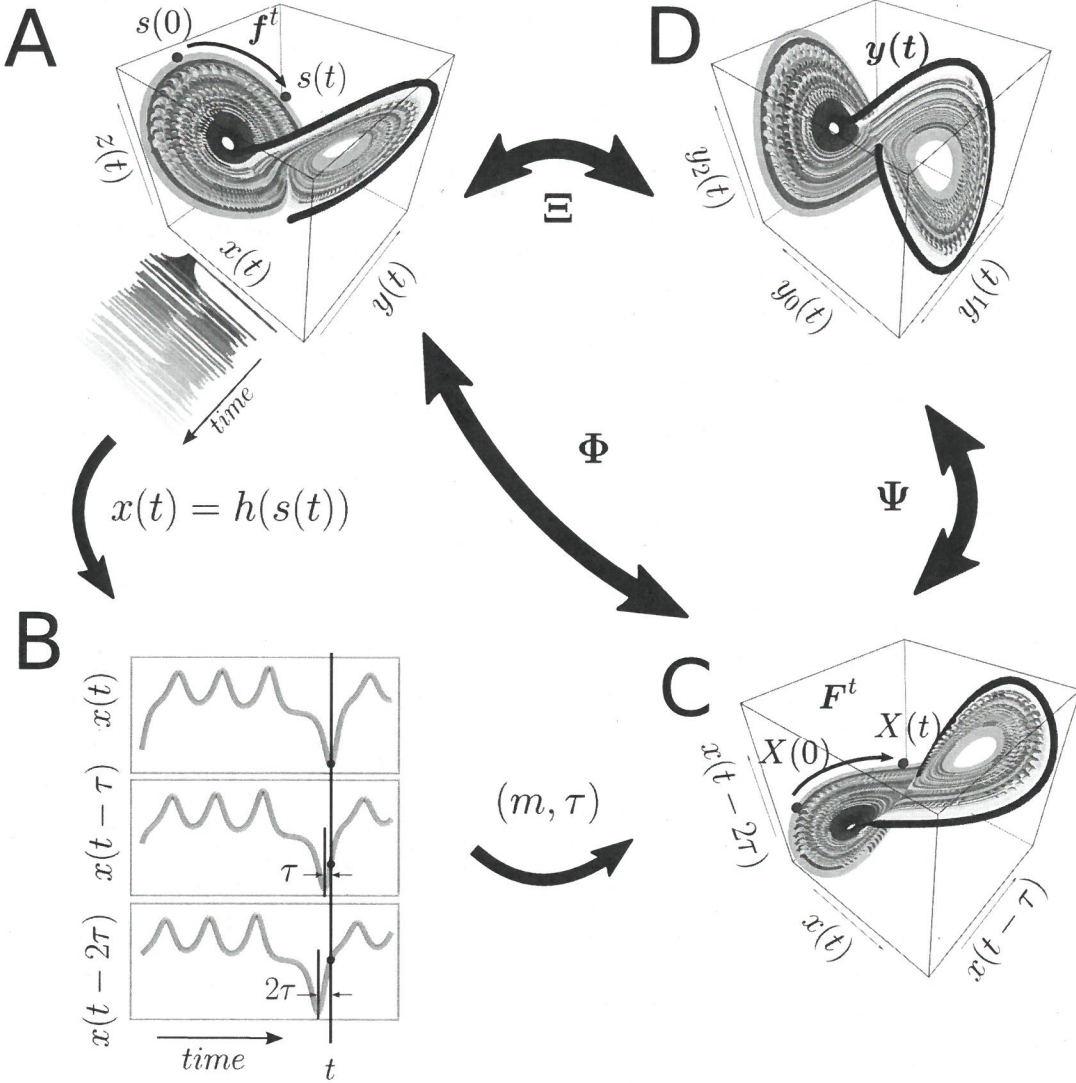


**Fig. 3.1 State space reconstruction methodology.** State space reconstruction is based on  $x(t) = h[s(t)] = h[f^t[s(0)]]$  where  $h[\cdot]$  is a function  $h : M \rightarrow \mathbb{R}$ , defined on the trajectory  $s(t)$ .  $f$  is the true dynamical system,  $f : M \rightarrow M$ , defined as evolution function and  $f^t$ , with time evolution  $t \in \mathbb{N}$  which is the  $t$ -th iteration of  $f$  that corresponds to an initial position  $s(0) \in M$ . The time-delay embedding represented as the  $\Phi$ , maps the original  $d$ -dimensional state  $s(t)$  into the  $m$ -dimensional uniform time-delay embedding matrix  $\mathbf{X}(t)$ . The transformation map  $\Psi$  maps  $\mathbf{X}(t)$  into a new state  $y(t)$  of dimensions  $n < m$ . (A)  $M$ -dimensional state space (e.g. Lorenz system); (B) Delayed copies of 1-dimensional  $x(t)$  from the Lorenz system; (C)  $m$ -dimensional reconstructed state space with  $m$  and  $\tau$ , and (D)  $y(t)$  is the  $n$ -dimensional reconstructed state space. The total reconstruction map is represented as  $\Xi = \Psi \circ \Phi$  where  $\Phi$  is the delay reconstruction map and  $\Psi$  is the coordinate transformation map. This figure is adapted from the work of Casdagli et al. (1991); Quintana-Duque (2012); Uzal et al. (2011) and R code to reproduce the figure is available from Xochicale (2018).

the uniform time-delay embedding matrix  $\mathbf{X}_\tau^m$ ,  $\mathbf{X}_\tau^m \in \mathbb{R}^{m \times m}$ , defined as

$$\mathbf{X}_\tau^m = \begin{pmatrix} \tilde{\mathbf{x}}_n \\ \tilde{\mathbf{x}}_{n-\tau} \\ \tilde{\mathbf{x}}_{n-2\tau} \\ \vdots \\ \tilde{\mathbf{x}}_{n-(m-1)\tau} \end{pmatrix}^\top, \quad (3.4)$$

where  $m$  is the embedding dimension,  $\tau$  is the embedding delay and  $^\top$  denotes the transpose.  $m$  and  $\tau$  are known as embedding parameters. The matrix dimension of  $\mathbf{X}_\tau^m$  is defined by  $N - (m - 1)\tau$  rows and  $m$  columns and  $N - (m - 1)\tau$  defines the length of each delayed copy of  $\{\tilde{\mathbf{x}}_n\}$  in  $\mathbf{X}_\tau^m$ . A graphical representation of uniform time-delay embedding is shown in Figure 3.2. For further details and explicit examples of uniform time-delay embedding methodology, we refer the reader to the appendix A.

## 3.4 Estimation of Embedding Parameters

The estimation of the embedding parameters ( $m$  and  $\tau$ ) is an essential step for the state space reconstruction in order to apply the method of uniform time-delay embedding (UTDE). Hence, we review two of the most common algorithms, which will be used in this thesis, to compute the embedding parameters: the false nearest neighbour (FNN) and the average mutual information (AMI).

### 3.4.1 False Nearest Neighbours (FNN)

To select the minimum embedding dimension  $m_0$ , Kennel et al. (1992) used the method of false neighbours which can be understood as follows: on one hand, when the embedding dimension is too small to unfold the attractor (i.e. evolving trajectories in

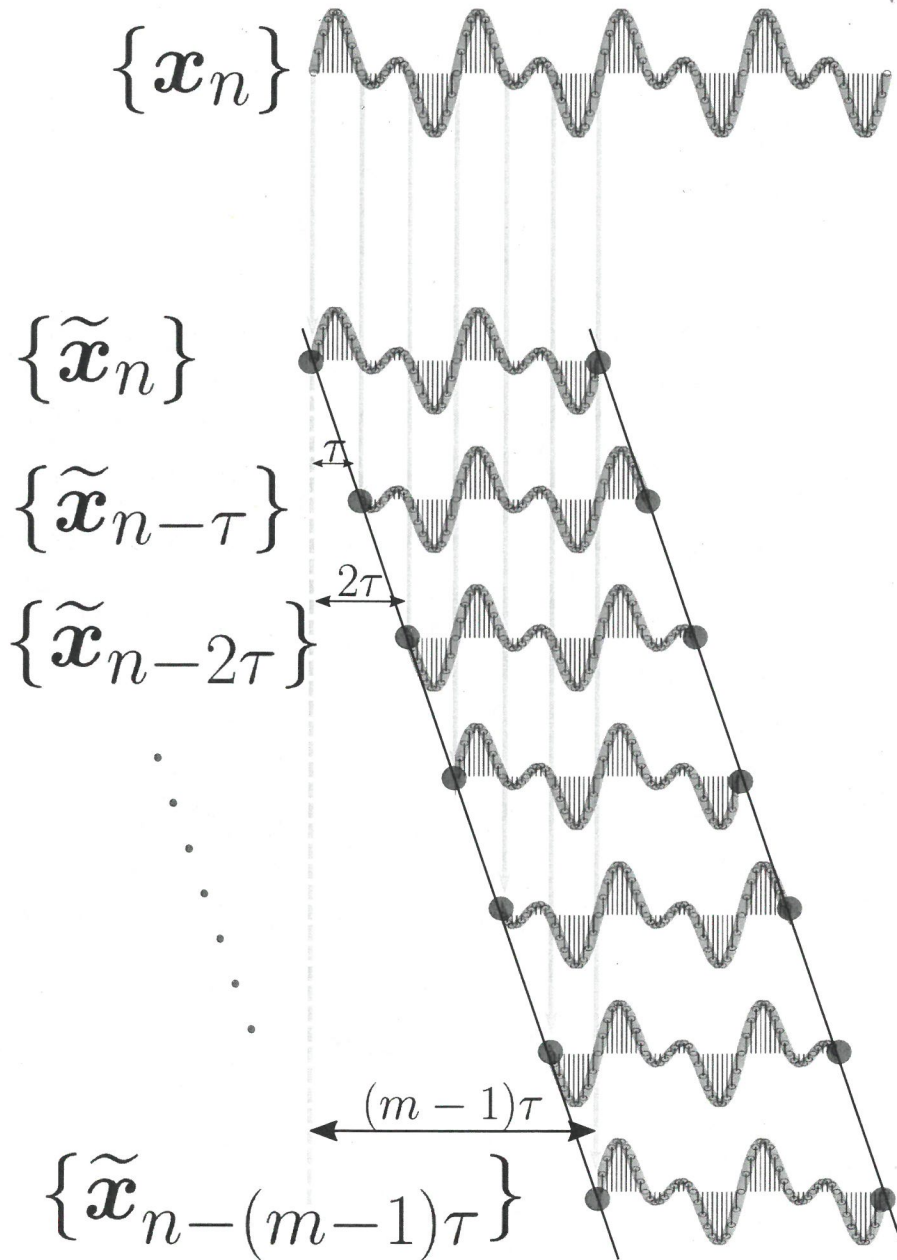


**Fig. 3.2 Uniform time-delay embedding.** UTDE is illustrated as  $m-1$  delayed copies of  $\{x_n\}$ , uniformly separated by  $\tau$  and represented as  $\{\tilde{x}_n, \dots, \tilde{x}_{n-(m-1)\tau}\}$  (Eq. 3.4). R code to reproduce the figure is available Xochicale (2018).

### 3.4 Estimation of Embedding Parameters

---

a state space) "not all points that lie close to each other will be neighbours and some points appear as neighbours as a result of the attractor being projected down into an smaller space", on the other hand, when increasing the embedding dimension "points that are near to each other in the sufficient embedding dimension should remain close as the dimension increase from  $m$  to  $m + 1$ " (Krakovská et al., 2015, p. 3).

From a mathematical point of view, state space reconstruction is done when the attractor is unfolded with either the minimum embedding dimension,  $m_0$ , or any other embedding dimension value where  $m \geq m_0$  (Kennel et al., 1992). In contrast, any large value of  $m_0$  leads to excessive computations (Bradley and Kantz, 2015). Hence, Cao (1997) proposed an algorithm based on the false neighbour method where only the time-series and one delay embedding value are necessary to select the minimum embedding dimension. Cao's algorithm is based on  $E(m)$ , which is the mean value of all  $a(i, m)$ , ~~with~~ defined as:

$$\begin{aligned} E(m) &= \frac{1}{N - m\tau} \sum_{i=1}^{N-m\tau} a(i, m) \\ &= \frac{1}{N - m\tau} \sum_{i=1}^{N-m\tau} \frac{\|\mathbf{X}_i(m+1) - \mathbf{X}_{n(i,m)}(m+1)\|}{\|\mathbf{X}_i(m) - \mathbf{X}_{n(i,m)}(m)\|} \end{aligned} \quad (3.5)$$

where  $\mathbf{X}_i(m)$  and  $\mathbf{X}_{n(i,m)}(m)$  are the time-delay embeddings with  $i = 1, 2, \dots, N - (m - 1)\tau$  and  $n(i, m) = 1 \leq n(i, m) \leq N - m\tau$ . From Eq. 3.5  $E(m)$  is only dependent on  $m$  and  $\tau$  for which  $E_1(m)$  is defined as

$$E_1(m) = \frac{E(m+1)}{E(m)}. \quad (3.6)$$

~~describe~~  
 $E_1(m)$  is therefore proposed to ~~investigate~~ the variation from  $m$  to  $m + 1$  in order to find the minimum embedding dimension  $m_0$  (Eq. 3.6). As Cao 1997, p. 44 described: " $E_1(m)$  stops changing when  $m$  is greater than some  $m_0$ , if the time series comes from a multidimensional state space then  $m_0 + 1$  is the minimum dimension". Additionally,

## Nonlinear Analyses

---

Cao (1997) proposed  $E_2(m)$  to distinguish deterministic signals from stochastic signals.  $E_2(m)$  is defined as

$$E_2(m) = \frac{E^*(m+1)}{E^*(m)}, \quad (3.7)$$

where

$$E^*(m) = \frac{1}{N - m\tau} \sum_{i=1}^{N-m\tau} |\mathbf{X}_i(m+1) - \mathbf{X}_{n(i,m)}(m+1)|. \quad (3.8)$$

For instance, when the signal comes from random noise (values that are independent from each other), all  $E_2(m)$  values are approximately equal to 1 (e.g.  $E_2(m) \approx 1$ ). However, for deterministic data  $E_2(m)$  is not constant for all  $m$  (e.g.  $E_2(m) \neq 1$ ).

As an example of the use of  $E_1(m)$  and  $E_2(m)$  values, we consider two time series: the solution for the  $x$  variable of the chaotic deterministic Lorenz system (Figure 3.3E), and a Gaussian noise time series with zero mean and a variance of one (Figure 3.3F). We then compute  $E_1(m)$  and  $E_2(m)$  values for each time series. The  $E_1(m)$  values for the chaotic time series appear to be constant after the dimension is equal to six. The determination of six is given that any value of  $m$  can be used as  $E_1(m)$  values are within the threshold of  $1 \pm 0.05$  (Fig 3.3A). Although the  $E_2(m)$  values for the chaotic time series tend to be closer to one as  $m$  increases, these are different to one (Fig 3.3C), for which, it can be concluded that the chaotic time series comes from a chaotic deterministic signal. With regard to the noise time series,  $E_1(m)$  values appeared to be constant when  $m$  is close to thirteen which is defined by the same threshold of  $1 \pm 0.05$  (Figure 3.3B). Then, contrary to the  $E_2(m)$  values for a chaotic Lorenz time series, all values of  $E_2(m)$  for a noise time series are approximately equal to one (Figure 3.3D). Hence,  $E_1(m)$  values then indicate the minimum embedding dimension of the noisy time series is thirteen, however all of the  $E_2(m)$  values are approximately equal to one (Figure 3.3D) for which it can be concluded that noise time series is a stochastic signal.

## Nonlinear Analyses

---

spread and uncorrelated which makes recovering the underlying attractor (i.e. evolving trajectories in a state space) difficult if not impossible (Casdagli et al., 1991; Emrani et al., 2014; Garcia and Almeida, 2005).

There are many approaches to compute the embedding parameters (Bradley and Kantz, 2015), for instance, geometry-based methodologies where the amount of space filled in the reconstructed state is the metric to compute the delay embedding (Rosenstein et al., 1994) or theoretical approaches to estimate an optimal parameter for  $\tau$  Casdagli et al. (1991). However, the autocorrelation function and the average mutual information (AMI) are the two most commonly used algorithms to compute the minimum delay embedding parameter  $\tau_0$ . Emrani et al. (2014) used the autocorrelation function in which the first zero crossing is considered as the minimum delay embedding parameter. However, the autocorrelation function is a linear statistic whereas AMI considers the nonlinear dynamical correlations (Fraser and Swinney, 1986; Krakovská et al., 2015). With that in mind, the AMI algorithm is described below to estimate the minimum delay embedding parameter,  $\tau_0$ .

To compute the AMI, an histogram of  $x(n)$  using  $n$  bins is calculated and then a probability distribution of data is computed (Kantz and Schreiber, 2003). AMI is therefore denoted by  $I(\tau)$  which is the average mutual information between the original time series,  $x(n)$ , and the delayed time series,  $x(n - \tau)$ , delayed by  $\tau$  (Kabiraj et al., 2012). AMI is defined by

$$I(\tau) = \sum_{i,j}^N p_{ij} \log_2 \frac{p_{ij}}{p_i p_j}. \quad (3.9)$$

Probabilities are defined as follows:  $p_i$  is the probability that  $x(n)$  has a value inside the  $i$ -th bin of the histogram,  $p_j$  is the probability that  $x(n + \tau)$  has a value inside the  $j$ -th bin of the histogram and  $p_{ij}(\tau)$  is the probability that  $x(n)$  is in bin  $i$  and  $x(n + \tau)$  is in bin  $j$ . The AMI is measured in bits (base 2, also called shannons) (Garcia and Sawitzki, 2016; Kantz and Schreiber, 2003). For small  $\tau$  ( $\tau < 3$ ), AMI will be large (

### 3.4 Estimation of Embedding Parameters

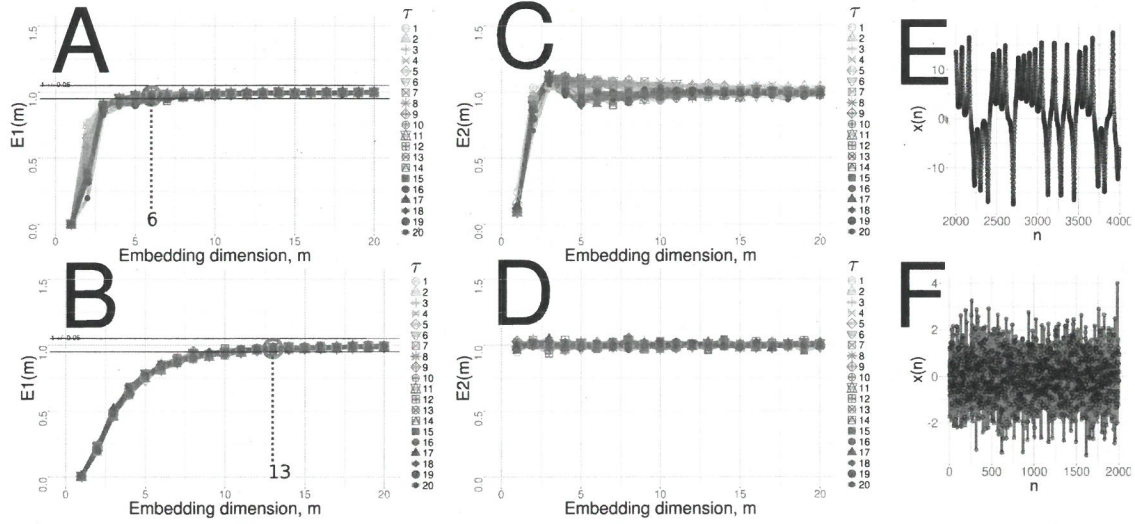


Fig. 3.3 Minimum dimension embedding values with Cao's method. (A, B)  $E_1(m)$  values and (C, D)  $E_2(m)$  values with variations of  $\tau$  values from one to twenty for (E) chaotic and (F) random time series. R code to reproduce the figure is available from Xochicale (2018).

It is important to note that for this thesis not only the values for  $E_1(m)$  and  $E_2(m)$  are computed but also a variation of  $\tau$  from 1 to 20 (Figure 3.3A,B,C and D) has been explored presented. The purpose of the increasing variations for  $\tau$  is to show its independence with regard to the  $E_1(m)$  and  $E_2(m)$  (Figure 3.3A,B,C, and D). Although Cao (1997) mentioned that no parameters are required to find the minimum embedding dimension, we found that it is necessary to define a new threshold for which  $E_1(m)$  values appear to be constant. Hence, for the given examples and the reported results for this thesis, we defined a threshold to be 0.05.

#### 3.4.2 Average Mutual Information (AMI)

When selecting the delay dimension parameter,  $\tau$ , one can consider the following two cases: (i) when  $\tau$  is too small, the elements of time-delay embedding will be along the bisectrix of the phase space and the reconstruction is generally not satisfactory, (ii) when  $\tau$  is too large the elements of the uniform time-delay embedding will become

### 3.4 Estimation of Embedding Parameters

$I(\tau) > 6$ ) and as  $m$  increase AMI will then decrease rapidly. Hence, as  $\tau$  increase and goes to a large limit,  $x(n)$  and  $x(n + \tau)$  have nothing to do with each other and  $p_{ij}$  is factorised as  $p_i p_j$  for which AMI is close to zero. Then, in order to obtain  $\tau_0$ , "it has to be found in the first minimum of  $I(\tau)$  where  $x(n + \tau)$  adds maximal information to the knowledge from  $x(n)$ " meaning that the redundancy between  $x(n + \tau)$  and  $x(n)$  is the least (Kantz and Schreiber, 2003, p. 151).

For example, we compute the AMI for two time series: (i) the  $x$  solution of the deterministic chaotic Lorenz system, and (ii) a noise time series using a normal distribution with mean zero and standard deviation equal to one. The AMI plots are shown in Figure 3.4, where the minimum delay embedding parameter for the chaotic time series is  $\tau_0 = 17$  and for the noise time series is  $\tau_0 = 1$ . Hence, it can be concluded that the amount of knowledge for any noise time series is zero for which the first minimum embedding parameter is equal to one. On the contrary, the first minimum of the AMI for the chaotic time series is  $\tau_0 = 17$  which is the value that maximize the independence in the reconstructed state space (Bradley and Kantz, 2015).

#### 3.4.3 Overall minimum embedding parameters

The method to select minimum embedding parameters ( $m_0$  and  $\tau_0$ ) for this thesis is firstly to compute  $m_0$  with FNN algorithm (considering a threshold of 0.05 for  $E_1(m)$  values), secondly to compute  $\tau_0$  with AMI which does not need any extra parameters. Hence, from the previous example of the chaotic deterministic Lorenz system, Fig 3.3(A) is used to determine the minimum dimension embedding ~~with a value of seventeen~~ ( $m_0 = 6$ ) and Fig 3.4(A) is used to determine the minimum delay embedding with a value of seventeen ( $\tau_0 = 17$ ). Therefore with the selection of the minimum embedding parameters, the reconstructed attractor is created in order to

[This could be explained a little more clearly. Are you suggesting to just read off figures 3.3A and 3.4A, or is there some additional calculation?]

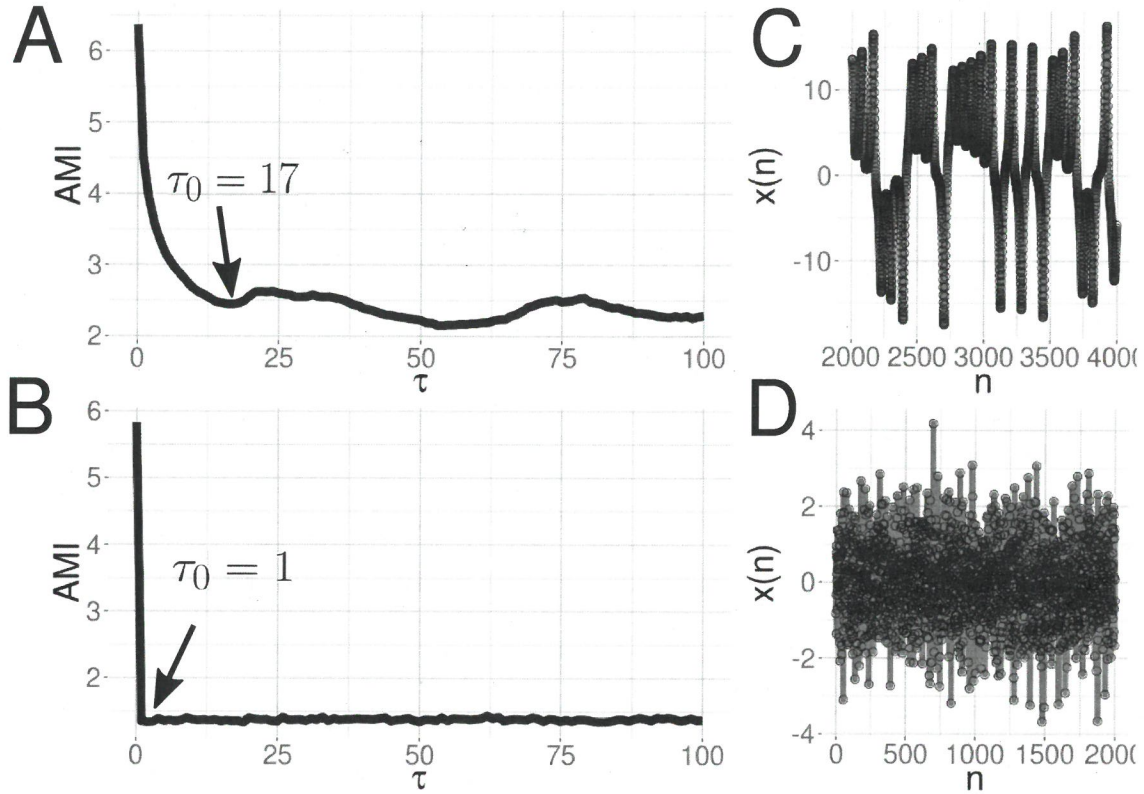


**Fig. 3.4 Minimum delay embedding values with AMI's method.** (A, B) AMI values where its first minimum value in the curve is the minimum time delay embedding ( $\tau_0$ ), for (C) a chaotic and (D) noise time series. R code to reproduce the figure is available from Xochicale (2018).

ensure with  $\tau_0$  the maximum independence between  $x(t)$  and  $x(t + \tau_0)$  and with  $m_0$  allowing the trajectories in the reconstructed state space to be unfolded.

We use sample mean for an overall value of embedding minimum embedding parameters  $(\bar{m}_0, \bar{\tau}_0)$  in which minimum values  $(m_{0_i}, \tau_{0_i})$  are averaged over  $N$  which is the total number of minimum embedding values:

$$\bar{m}_0 = \frac{1}{N} \sum_{i=1}^N m_{0_i}, \quad (3.10)$$

$$\bar{\tau}_0 = \frac{1}{N} \sum_{i=1}^N \tau_{0_i}. \quad (3.11)$$

## 3.5 Reconstructed State Space with UTDE

Given a time series  $x(n)$ , the UTDE matrix is computed with its minimum embedding parameters and then PCA is applied in order to select the first three axis of the rotated data to create the reconstructed state spaces (Frank et al., 2010; Samà et al., 2013).  
⇒ [perhaps show the final result of this process?]

## 3.6 Recurrence Plots (RP)

Henri Poincaré in 1890 introduced the concept of recurrences in conservative systems, however the discovery was not put into practice until the development of faster computers (Marwan et al., 2007), for which Eckmann et al. (1987) introduced a method where recurrences in the dynamics of a system can be visualised ~~using Recurrence Plots (RP)~~. The intention of ~~Eckmann et al.~~ Eckmann et al. (1987) was to propose a tool, called Recurrence Plot (RP), that provides insights into high-dimensional dynamical systems where trajectories are very difficult to visualise. Hence, "RP is a tool that helps us to investigate the  $m$ -dimensional phase space trajectories through a two-dimensional representation of its recurrences" (Marwan and Webber, 2015, p. 7). Similarly, Marwan and Webber (2015) pointed out that in addition to the methodologies of the state space reconstruction and other dynamic invariants (e.g. Lyapunov exponent, Kolmogorov-Sinai entropy), the recurrences of the trajectories in the phase space can provide important clues to characterise the underlying process for periodicities (as Milankovitch cycles) or irregular cycles (as El Niño Southern Oscillation). Such recurrences can not only be visualised using Recurrence Plots (RP) but also be quantified with Recurrence Quantification Analysis (RQA) metrics, which leads to applications of these tools in various areas such as Economics, Physiology, Neuroscience, Earth Science, Astrophysics and Engineering (Marwan et al., 2007).

## Nonlinear Analyses

---

A recurrence plot based on time series  $\{\mathbf{x}_n\}$  is computed from the state space reconstruction with uniform time-delay embedding method  $X(i) = \{\tilde{\mathbf{x}}_n, \dots, \tilde{\mathbf{x}}_{n-(m-1)\tau}\}$  where  $i = 1, \dots, N$ ,  $N$  is the number of considered states of  $X(i)$  and  $X(i) \in \mathbb{R}^m$  (Eckmann et al., 1987). The recurrence plot is therefore a two-dimensional  $N \times N$  square matrix,  $\mathbf{R}$ , where a black dot is placed at  $(i, j)$  whenever  $X(i)$  is sufficiently close to  $X(j)$ :

$$\mathbf{R}_{i,j}^m(\epsilon) = \Theta(\epsilon_i - \|X(i) - X(j)\|), \quad X(i) \in \mathbb{R}^m, \quad i, j = 1, \dots, N, \quad (3.12)$$

where  $N$  is the number of considered states of  $X(i)$ ,  $\epsilon$  is a threshold distance,  $\|\cdot\|$  a norm, and  $\Theta(\cdot)$  is the Heaviside function (i.e.  $\Theta(x) = 0$ , if  $x < 0$ , and  $\Theta(x) = 1$  otherwise) (Fig 3.5) (Eckmann et al., 1987; Marwan et al., 2007; Marwan and Webber, 2015). RP is also characterised with a line of identity (LOI) which is a black main diagonal line due to  $R_{i,j} = 1$  ( $i, j = 1, \dots, N$ ).

### 3.6.1 Structures of Recurrence Plots

Pattern formations in RPs can be designated either as topology for large-scale patterns or texture for small-scale patterns. In the case of topology, the following pattern formations are presented: (i) homogeneous where uniform recurrence points are spread in the RP e.g., uniformly distributed noise (Figure 3.6A), (ii) periodic and quasi-periodic systems where diagonal lines and checkerboard structures represent oscillating systems, e.g., sinusoidal signals (Figure 3.6B), (iii) drift where paling or darkening recurrence points away from the LOI is caused by drifting systems, e.g., logistic map (Figure 3.6C), and (iv) disrupted where recurrence points are presented white areas or bands that indicate abrupt changes in the dynamics, e.g. Brownian motion (Figure 3.6D) (Eckmann et al., 1987; Marwan and Webber, 2015). Texture, for small-scale patterns, can be categorised as: (i) single or isolated recurrence points that

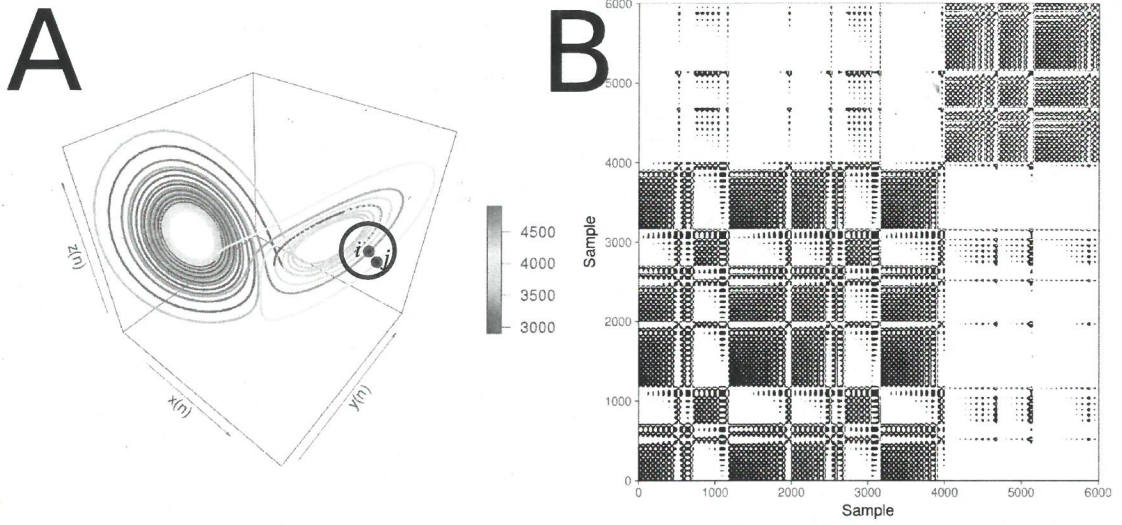


**Fig. 3.5 Recurrence Plots.** (A) State space of the Lorenz system with controlling parameters ( $\rho = 28, \sigma = 10, \beta = 8/3$ ). A point,  $j$ , in trajectory  $X()$  which falls into the neighborhood (black circle) of a given point at  $i$  is a recurrent point and is represented as a black dot in the recurrence plot at location  $(i, j)$  or white otherwise. (B) Recurrence plot using the three components of the Lorenz system and the RP with no embeddings and threshold  $\epsilon = 5$ . This figure is adapted from Marwan and Webber (2015) and R code to reproduce it is available from Xochicale (2018).

represent rare occurring states, do not persist for any time or fluctuate heavily, (ii) dots forming diagonal lines where the length of the small-scale parallel lines in the diagonal are related to the ratio of determinism or predictability in the dynamics of the system, and (iii) dots forming vertical and horizontal lines where the length of the lines represent a time length where a state does not change or change very slowly and the patterns formation represent discontinuities in the signal, and (iv) dots clustering to inscribe rectangular regions which are by related to laminar states or singularities (Marwan and Webber, 2015).

Although, each of the previous pattern descriptions of the structures in the RP offer an idea of the characteristics of dynamical systems from time-series, these descriptions might be misinterpreted and conclusions might tend to be subjective as these require the interpretation of a researcher(s). Because of that, recurrence quantification analysis

## Nonlinear Analyses

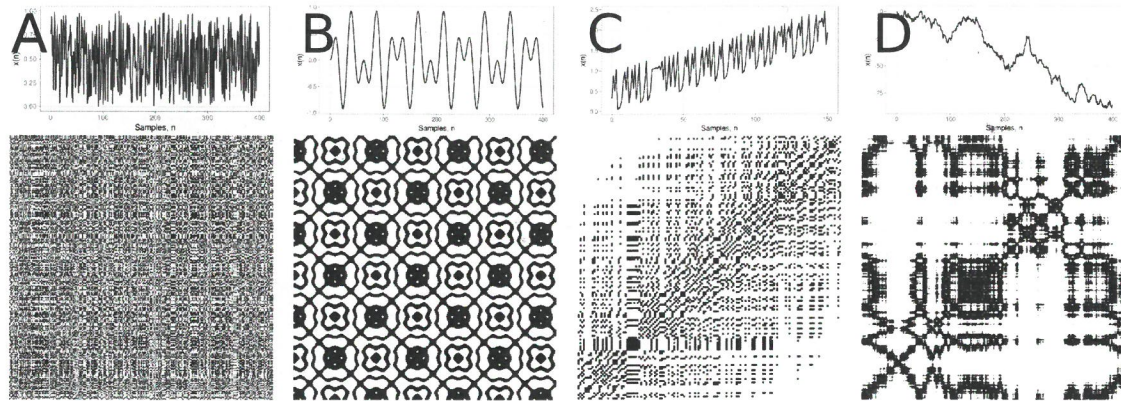


**Fig. 3.6 Patterns in Recurrence Plots.** Time-series with its respective recurrence plots for: (A) uniformly distributed noise, (B) super-positioned harmonic oscillation ( $\sin(\frac{1}{5} * t) * \sin(\frac{5}{100} * t)$ ), (C) drift logistic map ( $x_{i+1} = 4x_i(1 - x_i)$ ) corrupted with a linearly increase term ( $0.01 * i$ ), and (D) disrupted brownian motion ( $x_{i+1} = x_i + 2 * rnorm(1)$ ). Figure is adapted from Marwan and Webber (2015) and R code to reproduce the figure is available from Xochicale (2018).

(RQA) offer objective metrics to quantify the visual characteristics of recurrent pattern structures in the RP (Zbilut and Webber, 1992).

## 3.7 Recurrence Quantifications Analysis (RQA)

Zbilut and Webber (1992) proposed metrics to investigate the density of recurrence points in RPs, then histograms of lengths for diagonal lines in RPs were studied by Trulla et al. (1996), then Marwan (2008) introduced the term Recurrence Quantification Analysis (RQA). RQA metrics are percentage of recurrence, percentage of determinism, ratio, Shannon entropy of the frequency distributions of the line lengths, maximal line length and divergence, trend and laminarity (Marwan et al., 2007; Marwan and Webber, 2015).

### 3.7.1 Measures of RP based on the recurrence density

The percentage of recurrence (REC) or recurrence rate (RR) is defined as

$$REC(\epsilon, N) = \frac{1}{N^2 - N} \sum_{i \neq j=1}^N \mathbf{R}_{i,j}^m(\epsilon), \quad (3.13)$$

which enumerates the black dots in the RP excluding the line of identity. RR is a measure of the relative density of recurrence points in the sparse matrix (Marwan and Webber, 2015).

### 3.7.2 Measures of RP based on diagonal lines

The percent determinism (DET) is defined as the fraction of recurrence points that form diagonal lines and it is determined by

$$DET = \frac{\sum_{l=d_{min}}^N l H_D l}{\sum_{i,j=1}^N \mathbf{R}_{i,j}(\epsilon)}, \quad (3.14)$$

where

$$H_D(l) = \sum_{i,j=1}^N (1 - \mathbf{R}_{i-1,j-1}(\epsilon))(1 - \mathbf{R}_{i+l,j+l}(\epsilon)) \prod_{k=0}^{l-1} \mathbf{R}_{i+k,j+k}(\epsilon) \quad (3.15)$$

is the histogram of the lengths of the diagonal structures in the RP. DET can be interpreted as the predictability of the system for periodic signals which, in essence, have longer diagonal lines for chaotic signals shorter or absent diagonal lines for stochastic signals (Marwan et al., 2007; Marwan and Webber, 2015). Similarly, DET is considered as a measurement for the organisation of points in RPs (Iwanski and Bradley, 1998).

RATIO is defined as the ratio between DET and REC and it is calculated from the frequency distributions of the lengths of the diagonal lines. RATIO is useful to discover dynamic transitions (Marwan and Webber, 2015).

## Nonlinear Analyses

---

$D_{max}$  is the longest diagonal line in the RP, defined as

$$D_{max} = \arg \max_l H_D(l). \quad (3.16)$$

$D_{max}$  is an indicator of the divergence of trajectory segments. The smaller  $D_{max}$  is, the more divergent the trajectories are (Marwan et al., 2007; Marwan and Webber, 2015). According to Iwanski and Bradley (1998),  $D_{max}$  is also related to the inverse of the largest positive Lyapunov exponent, where for example periodic signals tend to have very long lines, as opposed to the chaotic time series where parallel lines are shorter.

The average diagonal line length is defined as

$$\langle D \rangle = \frac{\sum_{l=d_{min}}^N l H_D(l)}{\sum_{l=d_{min}}^N H_D(l)}, \quad (3.17)$$

and it is the average time that two segments of the trajectory are close to each other.  $\langle D \rangle$  can be interpreted as a measure for determinism (predictability) of the system (Marwan et al., 2007; Marwan and Webber, 2015).

ENT is the Shannon entropy of the frequency distribution of the diagonal line lengths and it is defined as

$$ENT = - \sum_{l=d_{min}}^N p(l) \ln p(l) \quad \text{with} \quad p(l) = \frac{H_D(l)}{\sum_{l=d_{min}}^N H_D(l)}. \quad (3.18)$$

ENT reflects the complexity of the deterministic structure in the system. For instance, for uncorrelated noise or oscillations, the value of ENT is rather small and indicates low complexity of the system, therefore "the higher the ENT is the more complex the dynamics are" (Marwan and Webber, 2015, p. 15).

### **3.7 Recurrence Quantifications Analysis (RQA)**

---

Trend (TND) "is a linear regression coefficient over the recurrence point density of the diagonals parallel to the LOI" (Marwan and Webber, 2015, p. 16) and is defined as

$$TND = \frac{\sum_{i=1}^{\tilde{N}} (1 - \tilde{N}/2)(RR_i - \langle RR_i \rangle)}{\sum_{i=1}^{\tilde{N}} (i - \tilde{N}/2)^2}. \quad (3.19)$$

Trend value "provides information about the stationarity versus nonstationarity in the process" (Marwan and Webber, 2015, p. 16). TNT values near to zero represent quasi-stationary dynamics and TNT values far from zero represent nonstationary dynamics that reveal the "drift in the dynamics" (Marwan and Webber, 2015, p. 16). TNT measures how quickly the RP pales away from the main diagonal (Iwanski and Bradley, 1998).

#### **3.7.3 Measures of RP based on vertical lines**

The previous RQA metrics are based on length, number and distribution of diagonal lines. However, patterns for horizontal and vertical lines can also be quantified. The following are some examples.

Laminarity (LAM) computes the percentage of recurrence points in vertical lines which is analogous to the DET variable Marwan and Webber (2015).

Trapping time (TT) variable computes the average length of vertical lines. "TT contains information about the amount and length of vertical structures in the RP" which represent "the mean time the system will" stay "at a specific time" (Marwan and Webber, 2015, p. 17).

The maximal length of the vertical structures  $V_{max}$  represents "the longest vertical line in the RP" which is analogous to  $D_{max}$ . According to Marwan et al. (Marwan and Webber, 2015, p. 17) the dynamical interpretation of this variable is not clear but only as a relationship with "singular states in which the system is stuck in a holding pattern inscribing rectangles in the RP".

### 3.7.4 The weakness and strengths of RP and RQA.

One of the main advantages of the use of RP is their capacity to detect small modulations in frequency or phase that are not detectable using standard methods e.g. spectral or wavelet analysis (Marwan, 2011). Nonetheless, RP is a very young field in nonlinear dynamics and many questions are still open, for instance, different parameters for window length size of the time series, embedding parameters or recurrence threshold can generate different results in RQA metrics (Eckmann et al., 1987; Marwan, 2011). Additionally, the selection of recurrence threshold,  $\epsilon$ , can depend on the system that is analysed. For instance, when studying dynamical invariants  $\epsilon$  require to be very small, for trajectory reconstruction  $\epsilon$  requires to have a large thresholds or when studying dynamical transition there is little importance about the selection of the threshold (Marwan, 2011). Other criteria for the selection of  $\epsilon$  is that the recurrence threshold should be five times larger than the standard deviation of the observational noise or the use of diagonal structures within the RP is suggested in order to find the optimal recurrence threshold for (quasi-)periodic process (Marwan, 2011).

Similarly, Iwanski and Bradley (1998) highlighted the importance of choosing the right embedding parameters to perform RQA for which many experiments have to be performed using different parameters in order to have a better intuition of the nature of the time series and how this is represented by using RQA. In the same investigation, Iwanski and Bradley (1998) pointed out that RQA metrics are quantitatively and qualitatively independent of embedding dimension. However, with an example, Iwanski and Bradley (1998) showed that two dissimilar RPs one from the Rössler system and the other from a sine-wave signal of varying period have got equal values of REC (2.1%) and have approximately equal values of DET (42.9%, 45.8%, respectively). Also, Iwanski and Bradley (1998) pointed out the importance of choosing the right parameters to perform RQA, since many experiments must be performed with different

### **3.7 Recurrence Quantifications Analysis (RQA)**

---

parameters to have a better intuition of the nature of the time series and how this is represented using RQA. Other example to determine embedding parameters for the RQA is the method of Zbilut and Webber (1992) in which 3D surfaces are created with an increase of embedding parameters ( $m$  and  $\tau$ ), then, for instance, Zbilut and Webber (1992) explored fluctuations and gradual changes in the 3D surfaces that provide information about the embeddings parameters. Recently, Marwan and Webber (2015) created 3D surfaces for visual selection of not only embedding parameters but also recurrence thresholds.

With that, therefore, it can be stated for this thesis that little has been investigated with regards to: (i) the strengthens and weaknesses of different nonlinear tools when using real-world data which is nonstationarity, noisy and has different sampling rate and length (Section 2.4), (ii) different models for movement variability where, for instance, not only the model of Stergiou et al. (2006) where complexity and predictability variables can characterise movement variability but also it can take into account the dependencies of the task dynamics (Vaillancourt and Newell, 2002, 2003) (Section 2.3.2), and (iii) the selection and application the right tools in order to quantify MV (Section 2.3.3). We, therefore, explore, in this thesis, the weaknesses and strengths of the window size of time series, embedding parameters for RSS with UTDE and recurrence threshold for RP and RQA in order to gain a better insight into the underlying time series collected from inertial sensors in the context of human-humanoid imitation activities.

⇒ *Summary*) Conclusions